Humidity-Dependent Bending Recovery and Relaxation of Human Hair

Franz J. Wortmann,[1] Michael Stapels,[2]* Lalitesh Chandra[3]

[1]*School of Materials, University of Manchester, Manchester, United Kingdom*
[2]*DWI e.V. and Institute of Technical and Macromolecular Chemistry, RWTH Aachen, Aachen Germany*
[3]*Unilever R&D, Port Sunlight, Wirral, United Kingdom*

Received 27 November 2008; accepted 25 February 2009
DOI 10.1002/app.30336
Published online 7 May 2009 in Wiley InterScience (www.interscience.wiley.com).

ABSTRACT: The time-dependent bending recovery of human hair fibers was investigated for a variety of relative humidities and aging times. The data were analyzed on the basis of a viscoelastic filament/matrix model and the Denby-equation, containing the parameter K as the ratio of the elastic bending rigidities of the matrix and the filaments and the Kohlrausch-Williams-Watts (KWW) function as relaxation function. The first stage of the analysis ascertained that the recovery curves shift with aging time on the time scale with the expected aging rate of $\mu \approx 1$. The second stage showed that the shape factor of the KWW function exhibits a mean value across the aging and humidity range of $m = 0.28$, which is close to the "universal" value of 1/3. On this basis, it was found that virtually no change occurs for the modulus ratio for low water contents up to about 10%, being constant at $K_0 = 6$ .1, while linearly decreasing beyond this threshold. The reduced, characteristic relaxation time drops on the log-time scale from $\log\tau_r(0) = 0.47$ for the dry fiber linearly with water content, covering about two thirds of a decade for 0–20% water content. With the pronounced humidity dependence of the parameters, hair shows what is termed hydro-rheologically complex (HRC) in analogy to thermo-rheologically complex behavior. Using the HRC approach, the dynamical mechanical performance of hair (1 Hz) was calculated for a range of water contents and aging times and found to be in good general agreement with experimental data. © 2009 Wiley Periodicals, Inc. J Appl Polym Sci 113: 3336–3344, 2009

Key words: α-keratin; human hair; bending recovery; filament/matrix composite; relaxation; aging; time/humidity superposition

INTRODUCTION

Hair is an appendage of the skin, which in various types grows basically on all parts of the body.[1,2] Head hair is generally about 50–90 μm in diameter, showing large differences in cross-sectional shape depending, mainly, on ethnic origin. Figure 1 shows a generalized, graphical representation of the complex morphological structure of a typical, keratin fiber.[3,4]

The hair fiber is constituted of cells that differentiate during hair growth. The cells at the core form the cortex whereas those at the periphery differentiate into flat, layered, structurally amorphous cuticle cells to form an outer protective layer of the fiber. The interface between the cells, the cell membrane complex (CMC), is a continuous phase of proteins and lipoproteins together with the adjacent membrane lipids. During hair growth, the cortex cells assume a spindle-like shape (length: approximately 100 μm, largest diameter: approximately 5 μm). The cortical cells express proteins that form as major cell component axially oriented, partial α-helical intermediate filaments (IF, diameter about 10 nm) embedded in an amorphous matrix of IF-associated proteins (IFAP). The IFAPs are highly cross-linked through cystine, which forms mainly interchain disulphide bonds.

For the context of mechanical or thermal investigations this complex structure can first be simplified as a three-phase, shell/core composite,[5] in which the shell is the cuticle and the core the cortex as a filament/matrix composite. Since the contribution of the cuticle toward mechanical properties is expected to be limited according to its low volume fraction (10–15%) and furthermore data on its mechanical properties are limited and conflicting,[6–8] this model is further simplified as a first-order approximation by the traditional two-phase, filament/matrix model, as originally proposed by Feughelman.[9] In this model the IF, or rather their α-helical fraction, are identified as the filamentous phase. The matrix in consequence contains as major component the amorphous IFAP[10] and also summarily the rest of the morphological components, such as cuticle, CMC,

Correspondence to: F. J. Wortmann (franz.wortmann@manchester.ac.uk).

**Present address:* Kao Chemicals Gmbh, Emmerich, Germany.

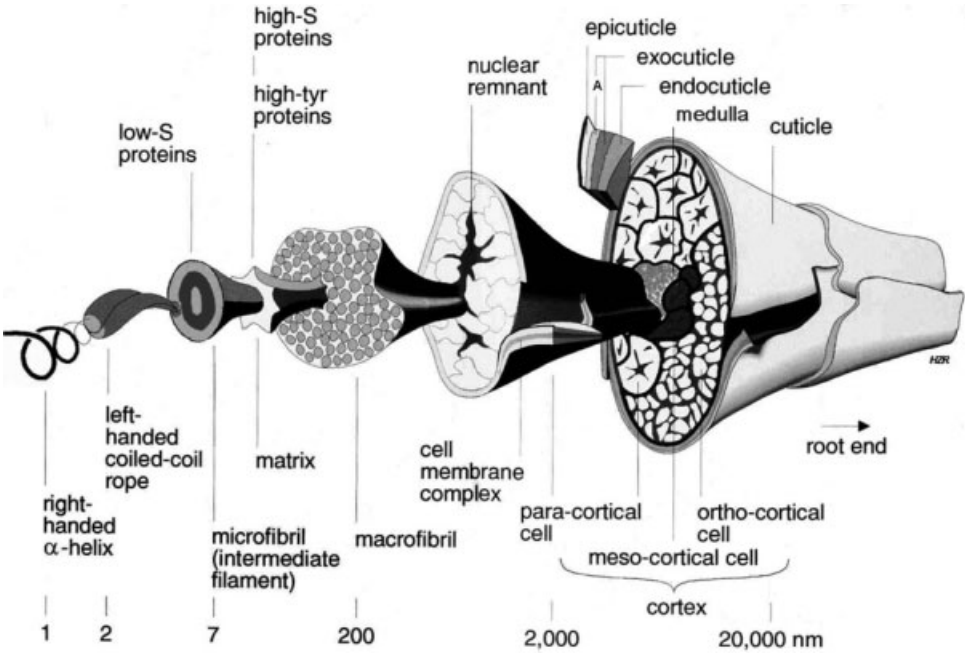

Figure 1 Generalized, graphical representation of the morphological structure of a typical α-keratinous fiber at progressive magnifications from right to left (Adapted from Refs. 3 and 4).

etc.[11] The matrix of keratins is an amorphous protein that exhibits a strongly humidity-dependent glass transition.[12,13] Under most practical conditions, such as 20°C and 65% relative humidity (rh), hair is a semicrystalline, viscoelastic,[14,15] glassy polymer.

In the daily consumer practice bending deformation, set and recovery under conditions of varying temperatures and humidities play an important role for the formation and stability of a hair style. Hair bending set is introduced by wetting and drying hair and is equivalent to bringing the deformed hair above its humidity-dependent glass transition temperature (T_G),[13] and then quenching it in the deformed state to below T_G, in analogy to an isothermal recovery experiment.[16] Accordingly, this set is removed on rewetting. For this type of set, occurring when a hair is styled by wetting and drying, Feughelman[3] has coined the term "cohesive" in contrast to "permanent" set, which occurs when hair is permwaved.[17] Cohesive set decreases with time. This is referred to as recovery and is attributed to the time-dependent breaking and reformation of hydrogen bonds in the hair proteins.

Against this background, it was the aim of our investigations to develop experimental and theoretical techniques to measure, model, and systematize the recovery performance of human hair fibers for isothermal conditions and for a range of relative humidity, to gain further insight into the relaxation behavior of human hair, including effects of physical aging. Here, we specifically report on experimental and theoretical investigations of the viscoelastic bending recovery of human hair at different relative humidities and states of physical aging.

EXPERIMENTAL

The ring test procedure applied by Wortmann et al.[17,18] in previous investigations to analyze the bending behavior of human hairs after permanent waving appeared to be best suited to determine the time-dependent bending recovery and relaxation of human hair under various relative humidities. Commercial, Caucasian mixed hair, untreated, medium brown (Kerling, Backnang, Germany) was used, taken at random from swatches (23 cm long).

The primary properties to be determined were time-dependent fiber bending set and recovery. For this, 3–4 fibers were wound around a 10 mm diameter glass cylinder each under a tension of 100 mg, and their ends fixed with fast glue (cyanoacrylate). The cylinder was immersed in distilled water for 15 min at 20°C, that is at conditions above T_G. Subsequently, the cylinder was removed from the water and dried for 5 min with a blow drier at 50°C, thus bringing the hairs rapidly to conditions below T_G. Because of the high ratio of cylinder versus fiber diameter, bending strains for the fibers are very small compared with 1% and therefore well within the limits of linear viscoelasticity for keratin fibers.[19]

The glass cylinder was stored for various aging times t_A between 10 min and 4000 min under controlled humidity conditions at 20°C. After this storage time, the fibers were cut along a line parallel to

TABLE I
Investigated Relative Humidity (rh) and Ageing Time (t_A) Combinations (20°C)

	rh, %					
t_A, min	15	33	45	65	74	82
10				x		
20				x		
30		x		x	x	
100		x		x	x	
250		x		x	x	
1000	x	x	x	x	x	x
1250				x		
2500		x			x	
4000				x		

the cylinder axis, each yielding 5–7 partially opened fiber rings for an individual fiber. All rings for a set of fibers were collected in a Petri dish, while preserving the conditions of storage. The recovery of each individual fiber segment from the ring form toward its initial straight shape was determined by measuring the diameters of the rings at fixed time intervals, roughly equally spaced for the log-time axis, and chosen with regard to the aging time of a given experiment. Table I summarizes the investigated combinations of relative humidity and aging time. Tests were generally conducted in triplicate. All experiments at 20°C and 65% relative humidity (rh) were carried out in a conditioned room. Other humidities (20°C) were generated in a glove box through the use of suitable saturated salt solutions[20] and controlled by a Digital Thermo-Hygrometer TH-1 (Carl Roth GmbH+Co, Karlsruhe, Germany).

The rings are formed through purely physical effects of their processing history as two-dimensional structures. Defining bending set as the retained fraction of initial bending deformation, it is readily shown[17] that the set S of the fiber at a given time t and at any point around the ring is related to the diameter d of the circle enclosing the partially opened ring by:

$$S(t) = d_0/d(t) \tag{1}$$

where d_0 is the diameter of the cylinder on which the fibers are initially wound. Set is related to recovery R, as the primary parameter to be used in this study, by:

$$R(t) = 1 - S(t) \tag{2}$$

DATA ANALYSIS

The variability of diameter and cross-sectional shape along as well as between hairs has a strong impact on absolute values for, e.g., bending stiffness (flexural stiffness, bending rigidity). Bending of a generally elliptical hair fiber will occur in practice with the long axis defining the neutral plane[21,22] so that bending rigidity B is given by:

$$B = E\,ab^3\,\pi/4 \tag{3}$$

where E is the elastic or Young's modulus, a the long, and b the short half-axis of the ellipse. In view of the strong influence of diameter on bending stiffness on the one hand and the high natural variability of the diameter and cross-sectional shape, the parameter of choice to study hair bending relaxation would thus ideally be normalized with respect to diameter.

Keratin fibers are linearly viscoelastic at low strains, that is generally below 1%.[14,19] By considering the deformation phase as part of the life-time of the material, Chapman[23] has shown that the formation of and the recovery from cohesive set in keratins follows the general principles of linear viscoelasticity, as based on the Boltzmann superposition principle.[24] Against this background Denby[25] developed an approximation to calculate the time-dependent recovery of a bent wool fiber from its relaxation performance that holds well for slow relaxation process, such as those considered here (Figs. 2 and 3), as:

$$R(t) = B(t)/B(t-\omega) \tag{4}$$

$B(t)$ is the time-dependent bending stiffness at any time after the initial deformation at $t = 0$. The fiber is released at $t = \omega$ and $B(t-\omega)$ is accordingly the bending stiffness of the same fiber, if it would have been bent at the time of release. Recovery is thus due to the antagonistic action of two bending

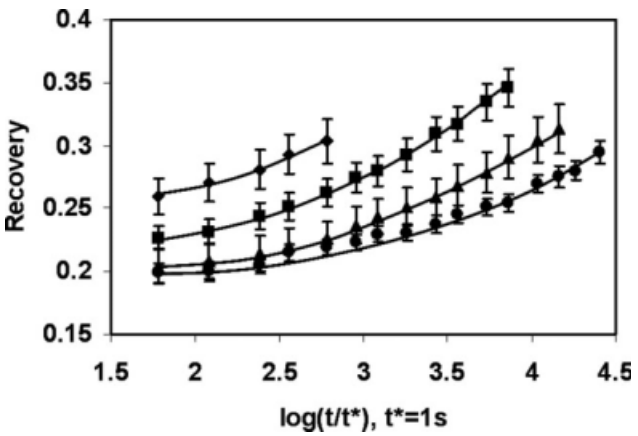

Figure 2 A family of recovery curves at 65% relative humidity and for various aging times t_A (◆ 20 min, ■ 250 min, ▲ 1000 min, ● 4000 min). The points are means for 8–41 individual measurements. The whiskers represent the standard errors for the arithmetic means. The lines are fitted through the data according to eq. (10).

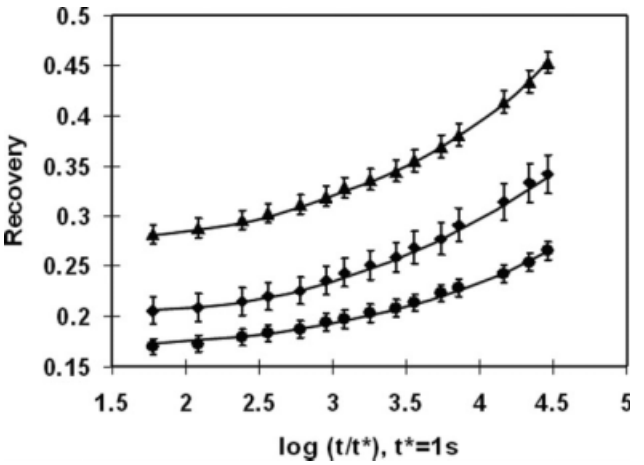

Figure 3 Examples of recovery curves recorded for different relative humidities (rh) (● 33%, ◆ 65%, ▲ 74%) at 20°C and equal aging time (t_A= 1000 min). Data points are means with standard errors (whisker). Lines are fitted through the data according to eq. (10).

rigidities. $B(t)$ relates to the straight fiber and tends to restraighten it, while $B(t-w)$ derives from the bent state of the same fiber and thus opposes redeformation. Equation (4) implies that the state of physical aging of the fiber during the recovery process remains unchanged. Since both variables act on the same cross-sectional area and shape, R becomes a normalized parameter, for which diameter related effects are canceled.

In an initial investigation[26] of bending recovery for a range of aging times and under standard conditions (65% rh, 20°C), it was established through graphical superposition of the curves that hair, similarly to wool,[14,23] shows changes of relaxation behavior with aging time t_A which are consistent with Struik's[27] effective time principle and with an aging rate of $\mu = 1$ [eq. (11) below]. That is, hair bending recovery curves shift on the log-time scale without changing their shape by one decade to higher times with every decade of increase in t_A.

One consequence of physical aging at a rate of $\mu = 1$ is that its effects will start to impact on the recovery curves at experimental times $t > 1/10\ t_A$ and will become of actual experimental relevance for slow changing curves, such as those in Figures 2 and 3, beyond $t > 1/3\ t_A$.[14] Data collection for the recovery curves were limited accordingly to a short-term experiment in Struik's[27] terminology ($t < 1/3\ t_A$), that is to experimental times which are small compared to the aging time, so that long-term effects of aging can be neglected.

In analogy to the case of extensional relaxation[14,19,28] time-dependent bending stiffness is described by:

$$B(t) = B_\infty + \Delta B \Psi(t) \tag{5}$$

with

$$\Delta B = B_0 - B_\infty \tag{6}$$

B_0 is the initial value of the bending rigidity at $t = 0$. B_∞ is the limiting, elastic stiffness reached by the fiber after complete physical relaxation. Ψ is the relaxation function. In the context of the two-phase model, B_∞ is the contribution of the elastic, partly α-helical filaments while ΔB is the limiting elastic contribution of the matrix, for which the viscoelastic behavior is described by $\Psi(t)$.

Previous investigations for α-keratinous materials[14,19,28,29] and various other polymers[30,31] have successfully made use of the cumulative log-normal distribution (CLND) as relaxation function. An obvious, practical disadvantage of the CLND function is the lack of an analytical form, necessitating the use of numerical approaches. However, this choice, following early considerations by Feltham,[32] meets requirements set by investigations of Kubat[33] for a strictly symmetrical relaxation function on the log-time scale, for the shape of which he also showed a marked material invariance.

A much more widespread and economical[34] choice for Ψ is, however, the stretched exponential of the Kohlrausch-Williams-Watts (KWW) function,[27,34,35] which shows an obvious relation to the non-specific Weibull distribution[36] on the one hand as well as to structural and molecular theories on the other.[37,38] Since in the current context, the differences between the functions are not overly pronounced,[39] the KWW-function is applied for these investigations as:

$$\Psi = \exp\left[-(t/\tau)^m\right] \tag{7}$$

where τ is the characteristic relaxation time and m the shape factor, which give the position and the width of the function on the log-time scale, respectively. The function is slightly skewed on the log-time scale.

The relaxation of the matrix contribution to the overall fiber bending stiffness is very fast in water,[15,28] where hair is well above its humidity-dependent glass transition.[13] This removes all effects of aging and yields effectively $\Delta B = 0$ after the wetting of the bent fibers during the initial step of the experiment. A substantial rubber elastic contribution to ΔB, as is expected from Hearle and Chapman's considerations,[40] was not observed in experiments by Druhala and Feughelman[41,42] and is thus neglected. Since this removes the time dependence of the numerator in eq. (4), the combination of eqs. (4) and (5) simplifies to:

$$R(t) = B_\infty/[B_\infty + \Delta B \Psi(t)], \quad t_A = \text{const} \tag{8}$$

where $t = 0$ is the start of the recovery experiment.

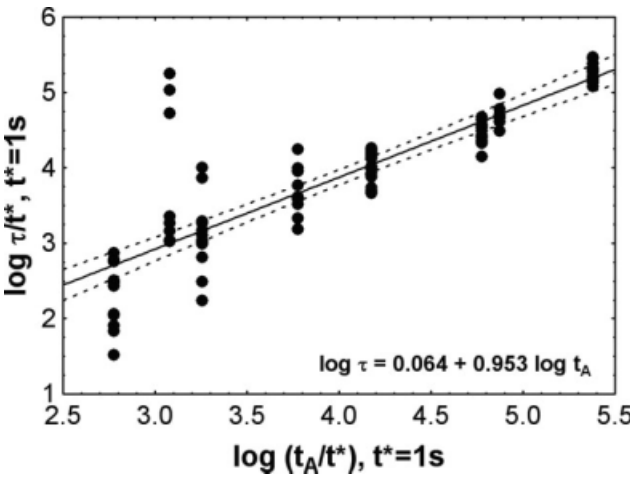

Figure 4 Characteristic relaxation times as log(τ) for individual recovery measurements at 65% rh /20 °C plotted *vs* the respective aging time as log(t_A). A straight line is fitted through the data and is given together with the 95% confidence limits for the means (broken lines). The slope of the solid line, as given by the inset equation, is statistically not significantly different from unity (95% level).

For the analysis of the experimental data eq. (8) is applied as:

$$R(t) = 1/[1 + K\Psi(t)] \tag{9}$$

where $K = \Delta B/B_\infty$ is the ratio between the elastic bending rigidities of the filaments and the matrix in the composite, respectively. Curve analysis was implemented by fitting the combination of eqs. (7) and (9) as

$$R(t) = 1/\{1 + K\exp[-(t/\tau)^m]\} \tag{10}$$

To data in the experimental time range $t < 1/3\ t_A$, applying nonlinear least-squares optimization, as e.g. implemented in Quattro Pro (Corel).

In the experiments, the hairs are rapidly brought from high to low water content through drying and are thus effectively quenched from conditions above to those below T_G. Ageing time t_A is defined as the time between the end of the drying process of the fiber loops and the point in time at which the fiber loops are cut open and recovery starts, which in turn is set to $t = 0$. In essence, this type of test is an isothermal recovery experiment at conditions below T_G[16] after rapid quenching.

RESULTS AND DISCUSSION

Figure 2 summarizes graphically recovery data for hairs at 65% rh) (20°C) and for different aging times between 20 min and 4000 min and the lines fitted through the data on the basis of eq. (10). Figure 3 gives an analogous view for curves for different relative humidities (20°C, $t_A = 1000$ min).

Fitting eq. (10) to all curves underlying Figure 2 yielded values for the characteristic relaxation time τ, presented versus aging time t_A on a log/log-scale in Figure 4. The straight line through the data has a slope of 0.953, which is statistically not significantly different from unity (95% level). Thus, log(τ) shifts synchronously with log(t_A) and confirms the value of the aging rate μ for a material well removed from thermodynamic equilibrium,[27] as:

$$\mu = d\log\tau/d\log t_A = 1 \tag{11}$$

In agreement with the results of Chapman obtained for wool[14,23] and by Struik[27] for a very diverse variety of materials in the range between the glass and the lower temperature β-transition.

Figure 5 summarizes the data obtained for the shape factor m by fitting eq. (10) to the recovery curves at 65%rh and for the various aging times in the form of a box-and-whisker plot. Figure 6 is the analogous presentation for curves at different relative humidities. Though some scatter of the values is observed, analysis of variance shows that for the whole data set differences are not statistically significant (95% level). This shows that the value of the shape factor m of the relaxation function Ψ in eq. (7) is independent of aging time and of humidity. Apparent deviations of m toward lower values, namely, for lower and higher humidities (Fig. 6) are attributed to compensation effects in the parameters.

For all curves an arithmetic mean of 0.282 ± 0.019 (95% confidence limits) is obtained, which is

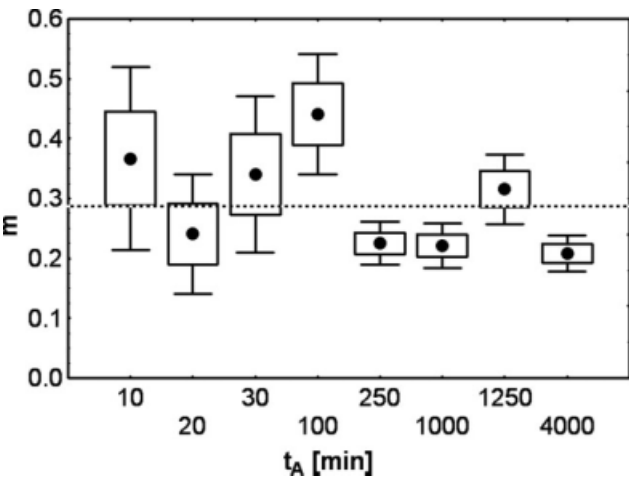

Figure 5 Shape factor m obtained by fitting eq. (10) to recovery curves at 65% rh and for different aging times. Data are summarized in the form of box-and-whisker plots (● mean, box: standard error, whisker: 95% confidence limits). The dotted line marks the overall mean for the data sets in Figures 5 and 6.

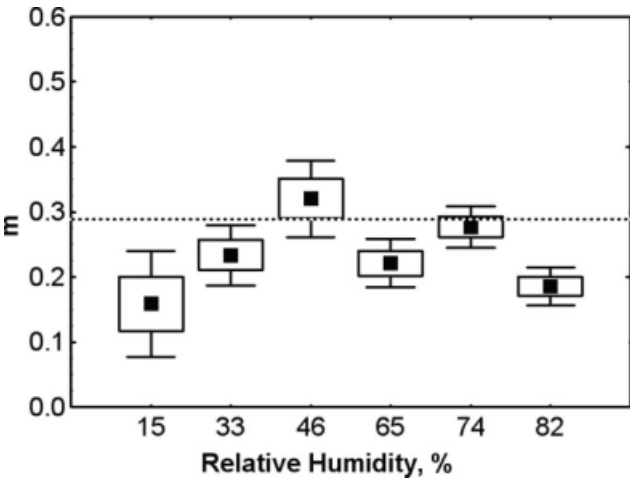

Figure 6 Shape factor m obtained by fitting eq. (10) to recovery curves at different relative humidities. Data are summarized in the form of box-and-whisker plots (■ mean, box: standard error, whisker: 95% confidence limits). The dotted line marks the overall mean for the data sets in Figures 5 and 6.

considered as being in good agreement with the limiting value obtained for conditions below T_G for the lysozyme/water system,[43] with the "universal" value of approximately 1/3 given by Struik[27] and the range of $m = 0.21$–0.35 found for various polymers by others (PVC, PP, PMMA, PS, PC[34,44]). Furthermore, it is consistent[39] with universal shape-factor value of the CLND-relaxation function for PTFE,[45] PP,[46] Kevlar, and Nomex.[47]

Since m was thus found to be constant over the investigated range of humidities and aging times, its value was restricted to its arithmetic mean to reduce compensation effects in the parameter values. Subsequently, the fits for the individual curves were performed again to yield values for the other parameters in eq. (10). As is to be expected from the applicability of the principles of physical aging, $K = \Delta B/B_\infty$ as the ratio of two elastic bending rigidities was found to be independent of aging time at all humidities, through unrestricted as well as restricted fits of eq. (10). Neither the modulus of the semicrystalline filaments nor the limiting modulus of the amorphous matrix change with aging time.

Having confirmed that K is independent of aging time, the relationship between K and humidity or rather water content of hair was investigated. The results for K are given in Table II and are graphically summarized in Figure 7. In view of the humidity independence of the modulus of the filaments, this is essentially the change of the limiting modulus of the matrix ΔB. The water content of hair for the various humidities was deduced from sorption isotherms for similar material.[48] The data and the graph show that virtually no change occurs for K for

TABLE II
K Values and Reduced, Characteristic Relaxation Times, as log τ_r, Given as Means with their 95% Confidence Limits ($q_{95\%}$)

rh (%)	w (%)	$K \pm q_{95\%}$	log $\tau_r \pm q_{95\%}$	N
15	4.0	5.9 ± 1.0	0.53 ± 0.124	15
33	7.8	6.2 ± 0.41	0.15 ± 0.048	173
45	9.5	6.2 ± 0.67	0.22 ± 0.071	28
65	13.0	4.7 ± 0.36	0.031 ± 0.0003	130
74	15.1	3.3 ± 0.19	−0.13 ± 0.042	160
82	17.3	2.4 ± 0.21	−0.01 ± 0.054	37

Parameter values were determined by fitting eq. (10) to the recovery curves with the restriction of $m = 0.282$. rh is the relative humidity and w the water content of hair. N is the number of individual curves analyzed.

water contents up to about 10%, equivalent to roughly 50% rh. The arithmetic mean over this range, representing the limiting value of K for low humidities, is $K_0 = 6.1 \pm 0.7$ (95% confidence range). For higher water contents K decreases linearly with water content, as has been observed for wool.[14]

In view of $K = \Delta B/B_\infty$ and the humidity invariance of B_∞ this would imply that the modulus of the matrix is much higher than that of the filaments and that it does not change in the low humidity range. This is in contrast to the observations for wool in extensional and torsional experiments[11,14,49] but in agreement with bending experiments on European human hair between 10 and 100% rh.[50] The effect can consistently[26] be attributed to limitation of the two-component model for hair in bending, namely, to the high modulus of the exo-cuticle at low to medium regains[6] in the thick, multilayer

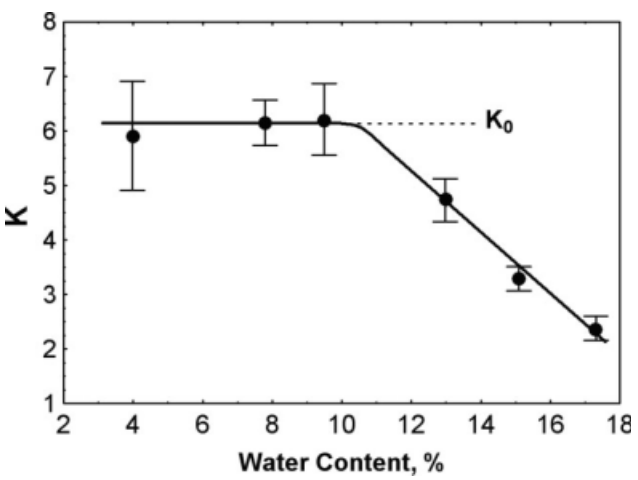

Figure 7 Parameter values for the rigidity ratio K *vs* water content, given as means (●) with their 95% confidence limits (whisker). The value of $K_0 = 6.1$, representing the arithmetic mean for water contents below 10%, is marked by the horizontal broken line, which connects to a sloped line beyond approx. 10% water content.

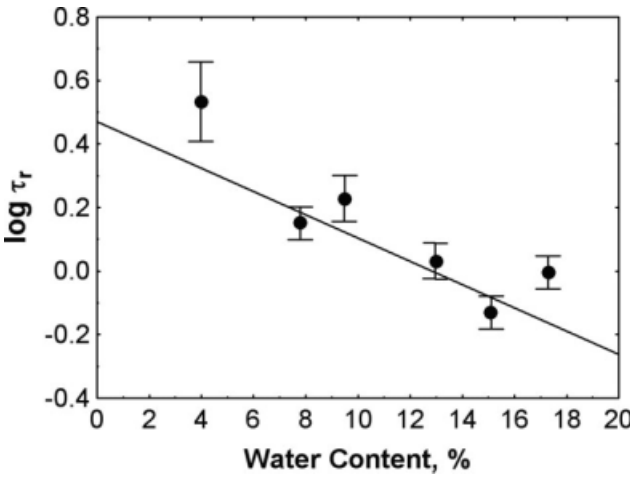

Figure 8 Parameter values for the reduced, characteristic relaxation time as log τ_r versus water content. The data are given as arithmetic means (●) together with their 95% confidence range (whisker). The line is the linear fit through the single values. The location of the regression line is largely controlled by the data in the mid range of water contents with large numbers of individual data.

cuticle-sheath surrounding the human hair, compared to a single cuticle layer in wool fibers.

To correct for the effects of aging at a given water content the parameter of the reduced, characteristic relaxation time τ_r is introduced:

$$\tau_r = \tau / t_A \tag{12}$$

so that

$$\log \tau_r = \log \tau - \log t_A \tag{13}$$

The results for log τ_r are given in Table II and are graphically summarized in Figure 8. The fit to the individual values, as given by the straight line in Figure 8, yields as limiting value for dry hair ($w = 0$) of log $\tau_r(0) = 0.47 \pm 0.089$ (95% confidence limits) and a slope of $d(\log \tau_r)/dw = -0.036 \pm 0.0072$ (95% confidence limits).

The parameter values drop over roughly two thirds of a decade from dry up to 20% water content, that is up to the glass transition at 20°C.[13] This is considerably smaller than the shift of the relaxation function for wool of well over on decade over the same range.[14] The overall small size of the shift of the relaxation time emphasizes the limited effect of water on the mobility on the protein chains in hair as well as the differences between human hair and wool, which can mainly be attributed to differences in the protein compositions of the matrix. The shifts are certainly much smaller than those over eight decades, which would have been expected from the universal behavior of a range of synthetic polymers.[51] But they are in good general agreement with the changes of water mobility in wool of about 1.5 decade between 25% rh and 100% rh as measured by NMR[52] and with the fact that all relaxations in hair investigated here occur at conditions below the glass transition.

Rearranging eq. (10) and isolating the time-dependent contribution of the matrix on the right-hand side of the equation yields:

$$1/R(t) - 1 = K \exp(-t/\tau_r)^m \tag{14}$$

which further leads to

$$\log[1/R(t) - 1] = \log K - (t/\tau_r)^m \tag{15}$$

with $m = 0.282$.

With the humidity dependencies of K and log τ_r it follows from eq. (15) that curves for log$(1/R-1)$ for different water regains w can be superimposed on the log/log scale onto a reference curve, which is characterized by the reference parameter values log K^{ref} and log τ^{ref}. Using the conventional notation this is done by horizontal shifts of:

$$-\log a_t(w) = \log \tau^{\text{ref}} - \log \tau(w) \tag{16}$$

and vertical shifts of

$$-\log a_K(w) = \log K^{\text{ref}} - \log K(w) \tag{17}$$

where $-\log a_t(w)$ and $-\log a_K(w)$ are the horizontal and the vertical shift, respectively, which are necessary to superimpose the curve at a given water content onto the reference curve on a log/log-scale.

The necessity of horizontal as well as vertical shifts on the log/log-scale to superimpose the transformed recovery curves, i.e. the relaxation function, is defined as hydro-rheologically complex (HRC) in

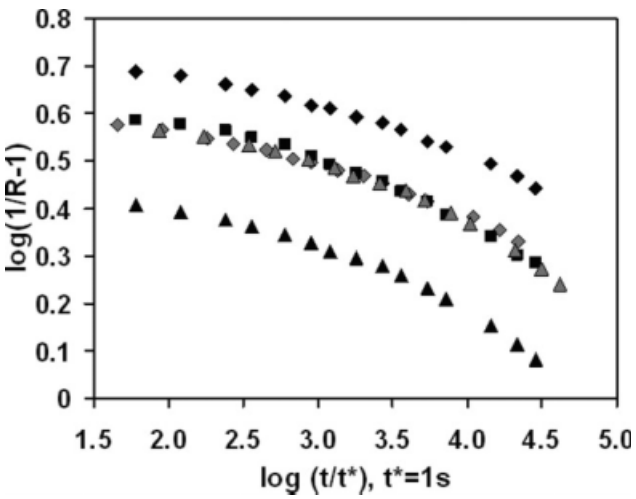

Figure 9 Recovery curves from Fig. 3 (t_A = 1000 min), transformed according to eq. (15) (◆ 33% rh, ■ 65% rh, ▲ 74% rh) and shifted vertically and horizontally (◆ 33% rh, ▲ 74% rh), according to eqs. (16) and (17) to superimpose onto the curve at 65% rh as reference curve.

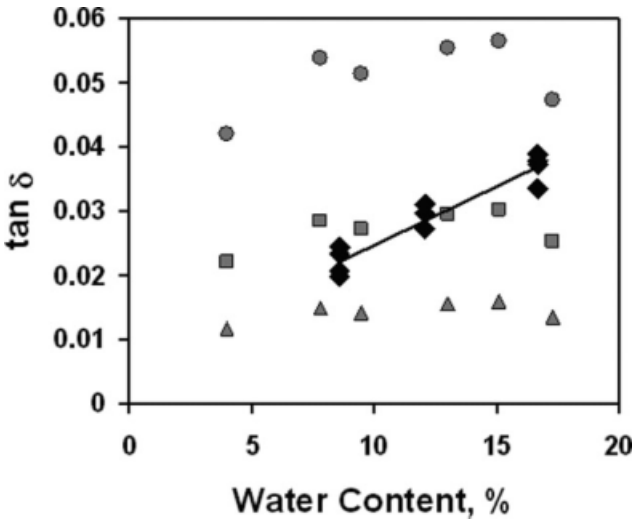

Figure 10 Values for tan δ calculated for a frequency of 1 Hz according to eq. (19) for various water contents, using the parameter values in Table II and assuming different aging times (● 10 min, ■ 100 min, ▲ 1000 min). Experimental values (◆) are taken from Ref. 54 with a straight line fitted through them.

analogy to thermo-rheologically complex behavior.[53] Figure 9 shows the transformed data from Figure 3 (t_A = 1000 min) superimposed onto the curve for 65% rh as reference curve. As was to be expected from the quality of the fits of eq. (10) to the curves, very good superposition is achieved.

To validate this approach dynamic mechanical performance, namely, tan δ is calculated and compared to experimental data[54] according to the common approximation[24]:

$$\tan\delta(\omega) = -\pi/2\; d\;\log\;[B(t)]/d\;\log\;(t)|_{t=1/\omega} \qquad (18)$$

From which follows with eqs. (8) and (10):

$$\tan\delta(\omega) = -\pi/2\, d\log\,[1/R(t)]/d\log\,(t)|_{t=1/\omega} \qquad (19)$$

where ω is the angular frequency.

Figure 10 gives the experimental data for tan δ determined by Jeong et al.[54] by dynamic mechanical analysis for natural and bleached Asian and Caucasian hair at one frequency (1 Hz) and three humidities. The water content of the hair at the humidities was inferred from the literature data.[48] Since the aging time of Jeong et al.[54] material is unspecified, data for tan δ were calculated applying eq. (19) and the parameter values for experimentally sensible aging times.

The results, summarized in Figure 10, show that the tan δ data show a tendency to increase with water content, which is related to the relatively small shift of the characteristic relaxation time to shorter times. The experimental data show good agreement with the calculated values for t_A = 100 min, as a sensible value for the unknown aging time underlying the experimental data. This result provides a good indicator for the consistency of the HRC approach. For the practical context of using dynamic mechanical analysis for testing hair for process and product development and claim support, it is important to note, however, that the differences between hair types and the effects of cosmetic processing are much smaller than the effects of physical aging that is of the humidity and thermal history of the hair fibers.

CONCLUSIONS

The ring test for human hair enabled the measurement of the viscoelastic bending recovery and thus effectively of the relaxation behavior for a range of humidities. The results reveal the effects of humidity on the elastic bending rigidity as well as on the relaxation performance of the matrix in the composite structure. These observations require the introduction of the principle of HRC behavior to arrive at successful superposition rules for the relaxation curves, which allow predictions for dynamic mechanical performance in accordance with experimental data. The differences, which are observed with respect to the HRC performance of human hair and wool, highlight the limitations of the two-component filament/matrix model for keratinous fibers, which will be the object of further investigations.

References

1. Robbins, C. R. Chemical and Physical Behavior of Human Hair; Springer: New York, 2002.
2. Jollès, P.; Zahn, H.; Höcker, H. Formation and Structure of Human Hair; Birkhaeuser: Basel, Switzerland, 1997.
3. Feughelman, M. Mechanical Properties and Structure of Alpha-Keratin Fibers; University of New South Wales Press: Sydney, Australia, 1997.
4. Marshall, R. C.; Orwin, D. F. G.; Gillespie, J. M. Electron Microsc Rev 1991, 4, 47.
5. Liu, H.; Bryson, W. G. J Text Inst 2002, 93, 121.
6. Parbhu, A. N.; Bryson, W. G.; Lal, R. Biochemistry 1999, 38, 11755.
7. Caldwell, J. P.; Bryson, W. G. Proc 11th Int Wool Conf, Leeds; UK, 2005; 89F.
8. Gibson, C. T.; Myhra, S.; Watson, G. S.; Huson, M. G.; Pham, D. K.; Turner, P. S. Text Res J 2001, 71, 573.
9. Feughelmann, M. Text Res J 1959, 29, 223.
10. Parry, D. A. D.; Steinert, P. Q. Rev Biophys 1999, 32, 99.
11. Zahn, H.; Wortmann, F.-J.; Wortmann, G.; Schaefer, K.; Hoffmann, R.; Finch, R. Ullmann's Encyclopedia of Industrial Chemistry, 6th ed; Wiley-VCH: Weinheim, Germany, 2003; Vol. 39, p 525
12. Wortmann, F. J.; Rigby, B. J.; Phillips, D. G. Text Res J 1984, 54, 6.
13. Wortmann, F. J.; Stapels, M.; Elliott, R.; Chandra, L. Biopolymers 2006, 81, 371.
14. Chapman, B. M. J Text Inst 1975, 66, 339.
15. Wortmann, F. J.; De Jong, S. Text Res J 1985, 55, 750.

16. Struik, L. C. E. Internal Stresses, Dimensional Instabilities, and Molecular Orientation in Plastics; John Wiley & Sons: New York, 1990; Chapter 5.
17. Wortmann, F. J.; Souren, I. J Soc Cosmet Chem 1987, 38, 125.
18. Wortmann, F. J.; Kure, N. J Soc Cosmet Chem 1990, 41, 123.
19. Wortmann, F. J.; De Jong, S. J Appl Polym Sci 1985, 30, 2195.
20. Greenspan, L. J Res Nat Bur Stand 1977, 81, 89.
21. Swift, J. A. Int J Cosmet Sci 1995, 17, 245.
22. Wortmann, F. J.; Schwan-Jonczyk, A. Int J Cosmet Sci 2006, 28, 61.
23. Chapman, B. M. Rheol Acta 1975, 14, 466.
24. Ferry, J. D. Viscoelastic Properties of Polymers; John Wiley & Sons: New York, 1980.
25. Denby, E. F. Rheol Acta 1975, 14, 591.
26. Stapels, M. Water waves in human hair. Investigation of the Basic Mechanics Controlling Formation and Recovery, PhD-thesis, RWTH-Aachen University, Aachen, Germany, 2002.
27. Struik, L. C. E. Physical Ageing in Amorphous Polymers and Other Materials; Elsevier: Amsterdam, NL, 1978; Chapter 4.
28. Wortmann, F. J. Colloid Polym Sci 1987, 265, 126.
29. Gupta, V. B.; Rao, D. R. J Appl Polym Sci 1992, 45, 253.
30. Wortmann, F. J.; Schulz, K. V. Polymer 1995, 36, 315.
31. Wortmann, F. J. Polymer 1999, 40, 1611.
32. Feltham, P. Br J Appl Phys 1955, 6, 26.
33. Kubat, J. Nature 1965, 205, 378.
34. Angell, C. A.; Ngai, K. L.; Mckenna, G. B.; McMillan, P. F.; Martin, S. W. J Appl Phys 2000, 88, 3113.
35. Alegria, A.; Colmenero, J.; Maro, P. O.; Campbell, I. A. Phys Rev E 1999, 59, 6888.
36. Fancey, K. S. J Polym Eng 2001, 21, 489.
37. Bendler, J. T.; Shlesinger, M. F. J Molec Liq 1987, 36, 37.
38. Phillips, J. C. J Non-cryst Solids 1994, 98, 172.
39. Wortmann, F. J. Forschungsber Land NRW; Westdeutscher Verlag: Opladen, Germany, 1992; Vol. 3245.
40. Hearle, J. W. S.; Chapman, B. M.; Senior, G. S. Appl Polym Symp 1971, 18, 775.
41. Feughelman, M.; Druhala, M. Proceedings of the 5th International Wool and Textile Research Conference, Aachen, Germany, 1976, II, 340.
42. Feughelman, M. Macromol Sci Phys 1979, 16, 155.
43. Pagnotta, S. E.; Gargana, R.; Bruni, F.; Bocedi, A. Phys Rev 2005, E71, 031506, 1.
44. Ngai, K. L.; Colmenero, J.; Alegria, A.; Arbe, A. Macromol 1992, 25, 6727.
45. Wortmann, F. J. Polymer 1996, 37, 2471.
46. Wortmann, F. J.; Schulz, K. V. Polymer 1996, 37, 819.
47. Wortmann, F. J.; Schulz, K. V. Polymer 1994, 35, 2108.
48. Wortmann, F. J.; Hullmann, A.; Popescu, C. IFSCC Mag 2007, 10, 317.
49. Bendit, E. G.; Feughelman, F. Encyclopedia of Polymer Science and Technology; Mark, H. F.; Gaylord, N. G., Eds. Interscience: New York, 1968; Vol. 8, p 1.
50. Scott, G. V.; Robbins, C. R. J Soc Cosmet Chem 1978, 29, 469.
51. Zhou, S. M.; Tashiro, K.; Ii, T. J Polym Sci Part B Polym Phys 2001, 39, 1638.
52. West, C. W.; Haly, A. R.; Feughelman, M. Text Res J 1961, 31, 899.
53. Schapery, R. A. Polym Eng Sci 1969, 9, 295.
54. Jeong, M.; Patel, V.; Tien, J. M.; Gao, T. J Cosmet Sci 2007, 58, 584.